USCAP

ARTICLE

Novel insights into the *BAP1*-inactivated melanocytic tumor

Michele Donati[1,2], Petr Martinek[3], Petr Steiner[3], Petr Grossmann[3], Tomas Vanecek[3], Liubov Kastnerova[2,3], Isabel Kolm[4], Martina Baneckova[2,3], Pietro Donati[5], Irina Kletskaya[6], Antonina Kalmykova[7], Josef Feit[8], Petr Blasch[9], Diana Szilagyi[10], Alfonso Baldi[11], Paolo Persichetti[12], Anna Crescenzi[1], Michal Michal[2,3] and Dmitry V. Kazakov[2,4]✉

BAP1-inactivated melanocytic tumor (BIMT) is a group of melanocytic neoplasms with epithelioid cell morphology molecularly characterized by the loss of function of *BAP1*, a tumor suppressor gene located on chromosome 3p21, and a mutually exclusive mitogenic driver mutation, more commonly *BRAF*. BIMTs can occur as a sporadic lesion or, less commonly, in the setting of an autosomal dominant cancer susceptibility syndrome caused by a *BAP1* germline inactivating mutation. Owing to the frequent identification of remnants of a conventional nevus, BIMTs are currently classified within the group of combined melanocytic nevi. "Pure" lesions can also be observed. We studied 50 BIMTs from 36 patients. Most lesions were composed of epithelioid melanocytes of varying size and shapes, resulting extreme cytomorphological heterogeneity. Several distinctive morphological variants of multinucleated/giant cells were identified. Some hitherto underrecognized microscopic features, especially regarding nuclear characteristics included nuclear blebbing, nuclear budding, micronuclei, shadow nuclei, peculiar cytoplasmic projections (ant-bear cells) often containing micronuclei and cell-in-cell structures (entosis). In addition, there were mixed nests of conventional and BAP1-inactivated melanocytes and squeezed remnants of the original nevus. Of the 26 lesions studied, 24 yielded a *BRAF* mutation, while in the remaining two cases there was a *RAF1* fusion. *BAP1* biallelic and singe allele mutations were found in 4/22 and 16/24 neoplasms, respectively. In five patients, there was a *BAP1* germline mutation. Six novel, previously unreported *BAP1* mutations have been identified. *BAP1* heterozygous loss was detected in 11/22 lesions. Fluorescence in situ hybridization for copy number changes revealed a related amplification of both *RREB1* and *MYC* genes in one tumor, whereas the remaining 20 lesions studied were negative; no *TERT-p* mutation was found in 14 studied neoplasms. Tetraploidy was identified in 5/21 BIMTs. Of the 21 patients with available follow-up, only one child had a locoregional lymph node metastasis. Our results support a progression of BIMTs from a conventional *BRAF* mutated in which the original nevus is gradually replaced by epithelioid BAP1-inactivated melanocytes. Some features suggest more complex underlying pathophysiological events that need to be elucidated.

Modern Pathology (2022) 35:664–675; https://doi.org/10.1038/s41379-021-00976-7

INTRODUCTION

BAP1-inactivated melanocytic tumor (BIMT) is a distinctive melanocytic neoplasm, nowadays listed in the WHO classification among combined nevi[1]. The rationale for such an interpretation is the identification of remnants of a conventional nevus with retained nuclear expression of BAP1 in many cases of BIMT that is otherwise mainly composed of BAP1-negative large epithelioid melanocytes with well-demarcated cytoplasmic borders and copious eosinophilic cytoplasm. From a molecular biological viewpoint, it is characterized by a *BRAF* mutation (or, rarely, *NRAS* mutation or *RAF1* fusion) considered to represent a mitogenic driver alteration and biallelic inactivation of the *BAP1* gene, leading to dysfunction of BAP1 protein[2–6].

BIMTs may occur at any age, with equal sex distribution and clinically present as a flesh-colored papule or nodule favoring the head and neck region, trunk, and upper extremities[7,8]. They occur sporadically or, less commonly, in the setting of an autosomal-dominant cancer susceptibility syndrome caused by a *BAP1* germline inactivating mutation that predisposes to uveal and cutaneous melanoma, mesothelioma, renal cell carcinoma, lung cancer, and several other neoplasms[9–13].

Most BIMTs seem to follow an indolent clinical course but cases of *BAP1*-inactivated melanomas have been reported,[8,10,14–17] suggesting a possible progression into an aggressive neoplasm. For lesions with atypical features, the term "melanocytoma" has been proposed by the WHO classification; however, no clear-cut criteria are established[1].

Albeit most BIMTs microscopically manifest peripherally located residua of a conventional nevus, occasional neoplasms are exclusively composed of large epithelioid melanocytes[5]. Other

[1]Department of Pathology, University Hospital Campus Bio-Medico, Rome, Italy. [2]Sikl's Department of Pathology, Medical Faculty in Pilsen, Charles University in Prague, Pilsen, Czech Republic. [3]Bioptical Laboratory, Pilsen, Czech Republic. [4]Department of Dermatology, University Hospital of Zurich, Zurich, Switzerland. [5]New Cytology Laboratory, Roma, Italy. [6]Russian Children's Clinical Hospital of Pirogov Russian National Research Medical University of the Ministry of Healthcare, Russian Federation, Moscow, Russia. [7]Laboratory of Pathology, CSD Health Care, Ltd., Kyiv, Ukraine. [8]Institute of Pathology, University of Ostrava, Ostrava, Czech Republic. [9]Department of Pathology, Regional Hospital, Hranice, Czech Republic. [10]Department of Pathology, Emergency Clinical County Hospital "Pius Brinzeu", Timisoara, Romania. [11]Department of Environmental, Biological and Pharmaceutical Sciences and Technologies, University of Campania "Luigi Vanvitelli", Caserta, Italy. [12]Department of Plastic, Reconstructive and Aesthetic Surgery, Campus Bio-Medico di Roma University, Rome, Italy. ✉email: kazakov@medima.cz

Received: 4 August 2021 Revised: 10 November 2021 Accepted: 10 November 2021
Published online: 2 December 2021

reported microscopic variations include binucleation and multinucleation of epithelioid cells, conspicuous lymphocytic infiltrate, small epithelioid melanocytes, rhabdoid cells, clear cells, and neoplasms with a conventional nevus-like morphology, suggesting a wider spectrum of histological presentation[7,8,10,18–20].

In fact, in our practice, we observed some hitherto underrecognized microscopic features, especially regarding several types of multinucleated/giant epithelioid melanocytes, nuclear characteristics (nuclear blebbing, nuclear budding, micronuclei, shadow nuclei), cell-in-cell structures (entosis), and other features that suggest more complex underlying pathophysiological events. We hereby report a clinical, morphological, and molecular analysis of 50 BIMTs, extending the morphological and mutational spectrum of the neoplasm.

MATERIALS AND METHODS

Case Selection

All 50 BIMTs from 36 patients were identified prospectively and retrospectively from the institutional and referral databases of the authors from 2004 to 2020. The inclusion criteria were the typical microscopic features with the loss of BAP1 nuclear staining on epithelioid melanocytes detected immunohistochemically. Clinical follow-up was obtained from the patients, their physicians, or from referring pathologists. Four cases have been previously reported[4,21].

Microscopic assessment

Histological features were individually assessed by two dermatopathologists (D.V.K. and M.D.).

The assessment parameters included the silhouette of the lesion (polypoid, verrucous, dome-shaped, or flat), symmetry, tumor thickness (Breslow index), type of lesion (combined one, that is having residua of a conventional nevus or "pure" one which is exclusively composed of BAP1-inactivated melanocytes), epidermal changes (irregular hyperplasia, atrophy/consumption, ulceration, or irritation), junctional component (presence and extension of BAP1-inactivated melanocytes), dermal growth pattern (nodular, sheet-like, nests, trabecular arrangement, areas with dyscohesive growth), cytological features, degree of nuclear pleomorphism, mitotic rate and mitoses distribution, cellular maturation, adnexal, vascular or perineural extension, lymphocytic infiltrate (scarce to absent versus moderate to heavy) and stromal changes (mucin deposits, melanin deposits, adipocytic metaplasia, presence of prominent fibrosis). While accessing cytological characteristics, we encountered and detected changes reported in the context of senescence, and cell-in cell structures (entosis).

Immunohistochemical studies

Immunohistochemical staining for BAP1 was mostly performed initially at the time of the diagnosis (in a few cases retrospectively) but were repeated for consistency using BAP1 (C-4, Santa Cruz) 4-µm sections cut from formalin-fixed, paraffin-embedded (FFPE) tissue using Ventana Benchmark XT automated stainer (Ventana Medical System, Inc, Tucson, AZ), according to the manufacturer's protocol. Additionally, staining for tyrosinase, S100 (polyclonal, Ventana), and BRAF V600E (VE1, Ventana) were performed in all cases.

Molecular analysis

Sample preparation. The FFPE tissue from selected cases was evaluated by a pathologist and relevant blocks were selected for molecular genetic analyses. For next-generation sequencing (NGS) RNA-based analyses, the total nucleic acid was extracted using an FFPE DNA kit (with the modified protocol for total nucleic acid extraction, automated on Maxwell RSC 48 Instrument, Promega, Madison, Wisconsin, USA). For DNA-based methods, DNA was isolated using a DNA mini kit (Qiagen, Hilden, Germany). Purified DNA and RNA were quantified, using the Qubit Broad Range DNA and RNA Assays, respectively (Thermo Fisher Scientific, Waltham, Massachusetts, USA).

Sanger sequencing of BAP1. PCR amplification of the whole coding sequence using in-house designed primers and Sanger Sequencing of *BAP1* were performed. The primers and PCR conditions were reported elsewhere[22]. From eight patients, either peripheral blood or saliva was tested for germline *BAP1* mutations after obtaining the patient's written consent.

BAP1 *(3p21.1) copy number changes by fluorescence in situ hybridization (FISH)*. For the detection of *BAP1* loss, a ready-to-use BAP1/CCP3 FISH Probe kit (Cytotest Inc., Washington DC, Maryland, USA) was used. The FISH procedure was performed as described earlier[23]. One hundred randomly selected non-overlapping tumor nuclei were evaluated in all samples. *BAP1* gene loss was calculated as the number of cells with loss (only one specific signal) divided by the total number of nuclei counted. The test was considered positive when >45% of nuclei had gene loss (mean +3 standard deviation in normal non-neoplastic tissues).

BRAF *hotspot mutations*. Analysis of eight *BRAF* hotspot mutations using the *BRAF* 600/601 StripAssay (ViennaLab Diagnostics GmbH Vienna, Austria) with analytical sensitivity 1% of the mutated allele was performed according to the manufacturer's instructions.

Fusion detection

Fusion transcripts detection was performed using the FusionPlex Solid Tumor kit (ArcherDX Inc., Boulder, CO) and TruSight Tumor 170 (Illumina, San Diego, CA), both according to the manufacturer's instructions. The process of FusionPlex library preparation and sequencing was described previouslys[24] and the data analysis was performed using the Archer Analysis software version 6.2.1. The details of fusion detection using the RNA part of TruSight Tumor 170 are described below.

Mutation analysis and copy number variations (CNVs) using NGS

Two gene panels of similar content (Comprehensive Cancer Panel, Qiagen; and TruSight Tumor 170, Illumina) were used for mutation detection. For both kits, the quality of DNA was assessed using the FFPE QC kit (Illumina), whereas the quality of RNA was tested using Agilent RNA ScreenTape Assay (Agilent, Santa Clara, CA). DNA samples with Cq < 5 and RNA samples with DV200 ≥ 20 were used for further analysis.

The TruSight Tumor 170 kit DNA and RNA libraries were prepared according to the manufacturer's protocol, except for DNA enzymatic fragmentation using KAPA FragKit (KAPA Biosystems, Washington, MA). Sequencing was performed on the NextSeq 500 sequencer (Illumina) following the manufacturer´s recommendations. Data analysis was performed using the TruSight Tumor 170 application on BaseSpace Sequence Hub (Illumina). CNVs were reported from the TruSight Tumor 170 application and the internal cutoff for reporting was set at >1.5 or <0.5 fold change. DNA small variant filtering and annotation were performed using the cloud-based tool Variant Interpreter (Illumina). Custom variant filter was set up including only variants with coding consequences and The Genome Aggregation Database database (GnomAD)[25] frequency value <0.01. Known benign variants according to the ClinVar database[26] were excluded. The remaining subset of variants was checked visually and suspected artefactual variants were excluded.

Alternatively, a library of 271 cancer-related genes using Comprehensive Cancer Panel was constructed using 250 ng of DNA. The library was sequenced on Nextseq 500, aiming at average coverage 350× after deduplication of molecular barcodes to detect 10% allele frequency with 95% sensitivity. Variants were called using Qiagen's proprietary pipeline. Subsequently, the variants were filtered using the calculated limit of detection for each sample. Variants more frequent than 0.01 in the GnomAD database were excluded as were known benign variants according to the ClinVar database. The remaining subset of variants was checked visually, and suspected artefactual variants were excluded.

Two tumors from one patient with multiple lesions were tested using NGS with MelArray, which comprises analysis of 57 genes, including *BAP1*, and *BRAF*, CNVs, tumor mutation burden (TMB), and HLA-typing[27].

FISH for copy number changes of *RRB1, CCND1, MYB, MYC,* and *CDKN2A*

FISH analysis and interpretation for a four-probe assay targeting 6p25 (*RRB1*), 11q13 (*CCND1*), 6p23 (*MYB*), and CEP6 (Vysis, Abbot Molecular) and for a three-probe assay targeting 9p21 (*CDKN2A*), 8q24 (*MYC*), and CEP9 were used as previously described by Gerami el al.[28]. The probes were hybridized on 4 µm-thick FFPE tissue sections, and the number and localization of the hybridization signals were assessed in a minimum of 100 randomly selected interphase nuclei with well-delineated contours.

RESULTS

Clinical findings

The clinical results are summarized in Table 1.

There were 25 female and 11 male patients, with a mean age of 30.4 years (range 7–81 yrs, median 25 yrs). Eight patients (22%) had more than one BIMT. Two patients were first-degree relatives. Locations included the head and neck area ($n = 19$), trunk ($n = 24$), upper extremities ($n = 3$), and genital area ($n = 1$); in three cases location was not specified. The clinical presentation was a flesh-colored exophytic lesion in all cases, with a median size of 0.6 cm (range 0.2–1.2 cm). In some lesions, a peripheral pigmented rim was evident, like a halo reaction. A melanocytic nevus was suspected by clinicians in 16 cases, in six of which the presence of focal pigmentation was also specified. Other clinical diagnoses included hemangioma, histiocytoma, pigmented basal cell carcinoma, and fibroma. In 21 patients, personal history of malignancy was known, and the diagnoses included uveal melanoma ($n = 1$), cutaneous melanoma ($n = 5$), mesothelioma ($n = 1$), renal ($n = 3$), lung ($n = 3$), breast ($n = 1$), thyroid cancer ($n = 1$) and schwannoma of the cerebellopontine angle ($n = 1$). In 15 cases, family or personal history of malignancy was unknown.

Table 1. Main clinicopathological data.

Clinical data	Frequency
Gender distribution	
Male	11
Female	25
Age, yrs	
Range	7–81
Mean	30.4
Median	25
Size (mm)	
Range	0.2–1.2
Mean	0.6
Median	0.5
Location	
Head/Neck	19
Trunk	24
Upper extremities	3
Genital area	1
Unknown	3
Personal (p) or family (f) history of malignancies	
Multiple BIMTs (patients)	8
Uveal melanoma (p)	1
Cutaneous melanoma (p)	5
Mesothelioma (p)	1
Renal cell carcinoma (p&f)	3
Colorectal carcinoma (f)	3
Lung& bronchial cancer (p&f)	3
Prostata carcinoma (f)	2
Breast cancer (p)	1
Leukemia (f)	1
Schwannoma (p)	1
Thyroid cancer (p)	1
Renal cell carcinoma (f)	1
Gynecological malignancy, NS (f)	1
Unknown (f)	15
Follow-up (months)	
Range	6–106
Mean	34.3
Median	30

NS: not specified, p: personal history, f: family history.

All cutaneous tumors were completely excised. No lymph node enlargement was clinically evident at the time of diagnosis. Clinical follow-up was available in 21 cases (34.3 months; range 6–106 months). All but two patients were alive and well without recurrence or metastasis). Two patients with the adverse clinical course included a 7-year-old girl with a family history of melanoma and a lesion on the lower neck developed a nodal metastasis in the ipsilateral triangular muscular space lymph node 6 years after the excision of the primary tumor; 8 years later after the onset of the disease, she underwent surgery for a second BIMT. Presently, she has no evidence of disease at the 8-year follow-up. The other patient also presented with multiple lesions and developed local recurrence in the scar (time after surgery remained unknown).

Histopathological findings

The accessed histopathological features are summarized in Table 2. The most common microscopic presentation was a predominantly dermally based melanocytic neoplasm with a dome-shaped or polypoid silhouette and an uneven, flat, or wedge-shaped base. A bulb-like deep extension was observed in nine cases. The mean Breslow thickness was 3.1 mm (range from 0.4 to 11 mm).

Most neoplasms ($n = 45$, 90%) were associated with the remnants of a conventional melanocytic nevus (combined BMITs), whereas five lesions (10%) were exclusively composed of BAP1-negative epithelioid melanocytes (pure BMITs). In most combined lesions, the remnants of conventional nevus were a minor component, usually situated at the periphery of neoplasm, as intact pre-existing nests or nests being surrounded and infiltrated by epithelioid melanocytes, resulting in mixed nests (Fig. 1). There were congenital ($n = 26$, 52%) features (splaying of melanocytes between collagen bundles, adnexotropism) and, rarely, dysplastic-like features (bridging of the adjacent junctional nests of conventional and/or epithelioid melanocytes with or without concentric/lamellar fibrosis) ($n = 7$, 14%) (Fig. 2A). Dermal conventional melanocytes at the transitional area often appeared to be squeezed by growing epithelioid melanocytes ($n = 17$, 34%) that mainly formed large expansile nodules, often coalescing and producing sheet-like areas, merging with the residual conventional nevus. There were also well-defined nests composed of exclusively epithelioid melanocytes, sometimes infiltrated by lymphocytes "dissolving" them (Fig. 1C). Epithelioid melanocytes also often demonstrated a dyscohesive or trabecular growth and/or single-cell arrangement toward the periphery of the lesion.

The predominant cell population was comprised of round to oval epithelioid melanocytes with well-demarcated cytoplasmic borders. The nuclei of the epithelioid cells displayed extreme variability in size, ranging from small (size of lymphocyte or plasma cell) to large/giant (five times or more the size of lymphocyte/plasma cell), with an approximately equal mixture of small, medium-sized and large epithelioid cells in 20 cases (40%). Large epithelioid melanocytes clearly dominated in 14 cases (28%), whereas small epithelioid cells dominated in 16 (32%) cases (Fig. 2C). Akin to nuclei, the amount of the cytoplasm of the epithelioid cells was variable. In most cases (80%), the cytoplasm of epithelioid cells, irrespective of the size and shape (see below), contained micronuclei (1/3 or smaller compared to the main nucleus), sometimes detaching from the main nucleus. Often, cells with cytoplasmic protrusions resembling proboscis were seen (ant-bear cells), with nuclei or micronuclei at the end of the protrusions (Fig. 3B).

Table 2. Summary of the microscopic features in 50 *BAP1*-inactivated melanocytic tumors.

Feature	Frequency
Thickness	
Range	0.4–11 mm
Mean	3.1 mm
Silhouette	
Polypoid with collarette	19 (38%)
Verrucous	3 (6%)
Dome-shaped	27 (54%)
Flat	1 (re-excision) (2%)
Base/border	
Flat base	20 (40%)
Wedge-shaped base	20 (40%)
Deep extension (bulb)	9 (18%)
Pushing border	4 (8%)
Epidermal changes	
Epidermal hyperplasia (irregular)	9 (18%)
Epidermal atrophy/consumption (focal)	24 (48%)
Ulceration	0
Irritation	12 (24%)
Junctional component	
Basal BAP1-inactivated melanocytes	23 (46%)
Extensive junctional component	12 (24%)
Architecture and growth patterns	
Pure	5 (10%)
Combined	45 (90%)
Associated nevus	
Dysplastic features	7 (14%)[a]
Congenital features	26 (52%)[a]
Minimal residual nevus	18 (36%)
Mixed nests (with BAP1+ and BAP1− cells)	
Junctional	18 (36%)
Dermal	27 (54%)
Arrangement of large epithelioid melanocytes	
Nodular/sheet-like	43 (86%)
Nests	26 (52%)
Trabecules	43 (86%)
Discohesive (focal)	44 (88%)
Cytological features epithelioid melanocytes	
Large mainly (3 × type B melanocytes)	14 (28%)
Small mainly (1 × type B melanocytes)	16 (32%)
Equal	20 (40%)
Pleomorphism	
Mild	13 (26%)
Moderate	36 (72%)
Severe	0
Cellular morphology of epithelioid melanocytes	
Large Hodgkin-like	46 (92%)
Binucleated with mirroring nuclei (Reed-Sternberg-like)	47 (94%)
Clear lacunar-like cells/cytoplasmic vacuolization	35 (70%)
Multinucleated Popcorn/Coin-on- a-plate/ Wreath-like	49 (98%)
Apoptotic (Mummified cells)	39 (78%)
Signet ring/Rhabdoid cells	29 (58%)
Ghost cells	45 (90%)
Ball-in-mitts (Entosis)	38 (76%)
Micronuclei	40 (80%)
Spindled epithelioid cells (focally)	3 (6%)
Pigmented epithelioid cells	6 (12%)
Clear nuclear pseudoinclusions	28 (56%)
Eosinophilic nuclear pseudoinclusions	26 (52%)
Mitotic rate in epithelioid melanocytes	
≤2 mitoses/mm^2	45 (90%)
>2 mitoses/mm^2	5 (10%)
Mitoses near base	13 (26%)
Adnexal, vascular, or perineural extension	
Adnexal involvement	13 (26%)
Perineural arrangement	6 (12%)
Intravascular invasion	0
Stromal changes	
Melanin deposits	35 (70%)
Mucin deposits	5 (10%)
Adipocytic metaplasia	6 (12%)
Prominent vascular and/or sclerotic stroma	5 (10%)
Inflammatory response	
Absent to scarce	15 (30%)
Moderate to heavy	35 (70%)
Plasma cells	11 (22%)
Other	
"Squeezed" conventional melanocytes	17 (34%)
"Kissing" lymphocytes	47 (94%)
Impaired maturation (focal)	46 (92%)

[a]Three cases manifested both dysplastic-like and congenital-like features.

Apart from cell size variability, there were also variations in shapes and nuclear appearances within an individual lesion, accounting for certain pleomorphism. Rare cells with large irregular nuclei resembling blebbing were seen, as were large, mononuclear cells with clumped chromatin (Fig. 4A, B). There were cells exclusively composed of large eosinophilic cytoplasm with only a shadow/vestige of a nucleus (Fig. 4C). Rare apoptotic epithelioid melanocytes with large, smudged nuclei and ample dense eosinophilic cytoplasm resembling mummified cells were also commonly encountered ($n = 39$; 78%). Clear and/or eosinophilic nuclear pseudoinclusions were observed in over half cases, with rare cells containing both types of nuclear pseudoinclusions (Fig. 4C).

Multinucleated/giant epithelioid melanocytes were always evident in varying numbers. Most conspicuous were binucleated cells with mirroring nuclei occasioning a resemblance to Reed-Sternberg cells. Other multinucleated cells included wreath-like cells, popcorn cells, floret-like cells, and coin-on-a-plate cells. Akin to mononuclear epithelioid cells, the nuclei within multinucleated epithelioid cells and the amount of cytoplasm manifested marked variation in size (Fig. 5).

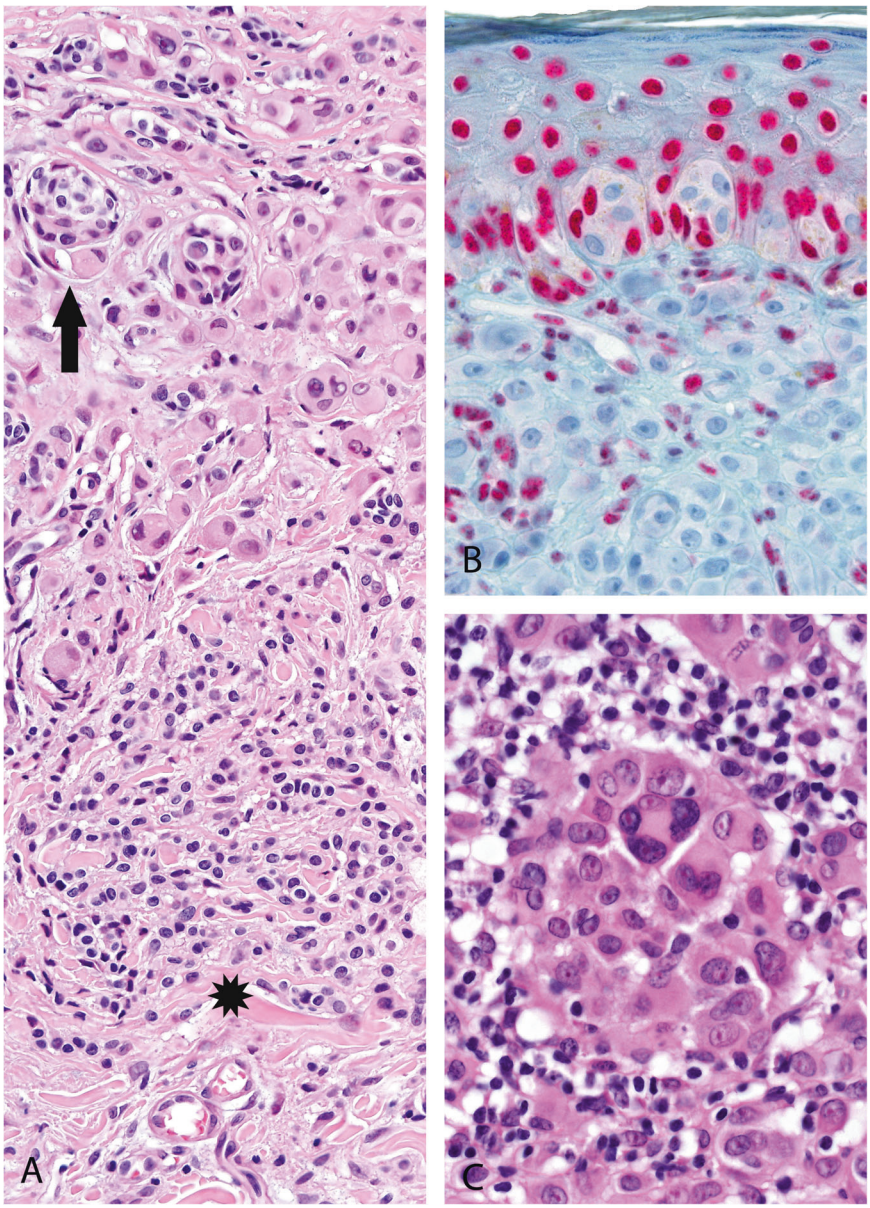

Fig. 1 Mixed and "dissoved" nests in BIMT. Remnants of conventional nevus with congenital features showing the splaying of melanocytes between collagen bundles (asterisk). Note the BAP1-inactivated epithelioid cells merging with conventional melanocytes wrapping around the nests, resulting in mixed nests composed of both conventional melanocytes and epithelioid cells (arrow) (**A**). Mixed nests composed of both BAP1-inactivated and BAP1-positive conventional melanocytes at the junction (**B**). A nest composed of exclusively BAP1-inactivated epithelioid melanocytes infiltrated by lymphocytes resulting in a dyscohesive growth pattern ("dissolved" nest) (**C**).

Prominent cytoplasmic vacuolization of occasional epithelioid cells resulting in a clear cell appearance was common ($n = 35$; 70%). There were also cells with an eccentric nucleus dislodged to the periphery by a large clear vacuole or abundant eosinophilic cytoplasm resembling so-called signet-ring cells or rhabdoid cells ($n = 29$; 58%). Other peculiar morphological aspects frequently noticed were cells with a lumina-like empty intracytoplasmic inclusion often encasing small to medium-sized melanocytes occasioning a resemblance to the so-called ball-in-mitt structures ($n = 38$; 76%) and likely representing entosis (Fig. 4D)[29,30].

In the majority of the cases ($n = 45$; 90%), the dermal mitotic count was ≤2 mitoses/mm^2. In four tumors, there were 5 mitoses/mm^2, and in one neoplasm 3 mitoses/mm^2 were seen. Mitotic figures near the base of the lesions were noted in 13 lesions (26%). Most lesions (96%) displayed at least focal impaired cellular maturation toward the base of the lesion were an admixture of small to medium-sized BAP1-inactivated cells, conferring a chaotic aspect or resulting in pseudomaturation. A moderate-to-heavy lymphocytic infiltrate was present in 35 cases (70%), usually with occasional lymphocytes lying in contact with the cell membrane of the BAP1-inactivated melanocytes. Plasma cells were noted in 11 cases (22%).

The epidermis showed focal atrophy and consumption in almost half the cases ($n = 24$; 48%), rarely in association with focal epidermal hyperplasia within the same lesion. In about a quarter of neoplasms, irritation was detected, while ulceration was never observed. Junctional BAP1-inactivated melanocytes were noted in 23 cases (46%) with extensive junctional involvement in 12 cases (24%). Lentiginous growth of epithelioid melanocytes within the basal cell layer of the epidermis was focally observed.

Rare findings (<15%) included intracytoplasmic melanin in epithelioid melanocytes, spindling of epithelioid melanocytes,

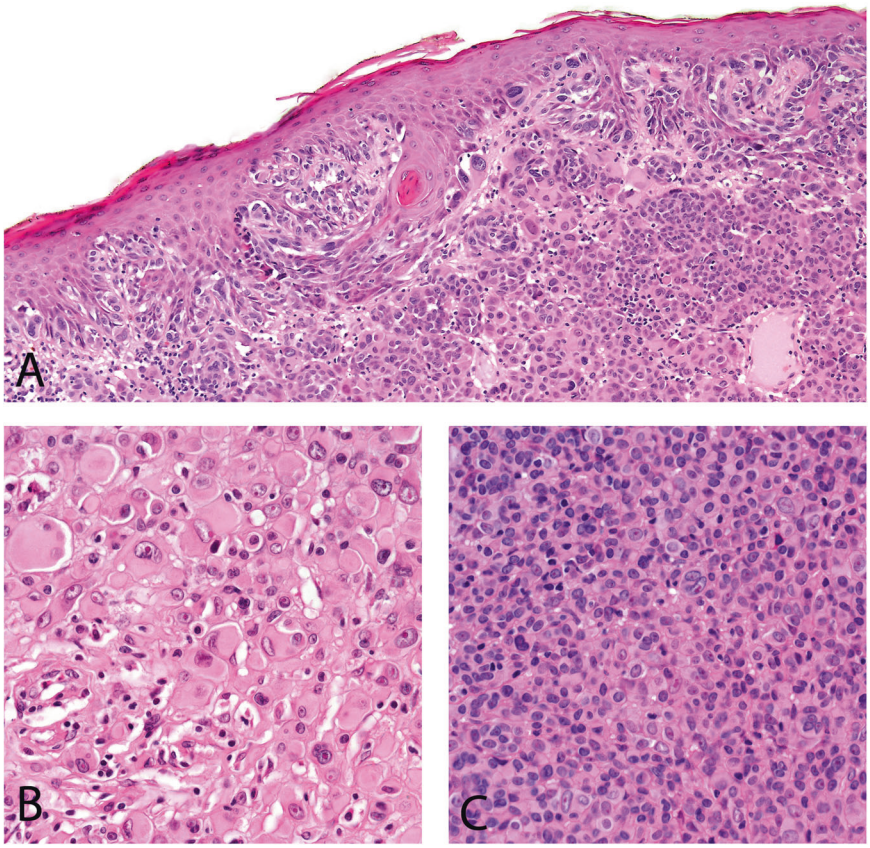

Fig. 2 Dysplastic-like features and cytological variations in BIMT. Bridging of the adjacent junctional, horizontally arranged nests of conventional and/or epithelioid melanocytes (**A**). Extreme cell size variability is a constant finding in BIMTs. Epithelioid melanocytes range from small (smaller than a lymphocyte) to giant cells (five times or more the size of lymphocyte/plasma cell) (**B**). BIMT mainly composed of small epithelioid melanocytes with eosinophilic cytoplasm and well-demarcated cellular border (**C**).

pigment incontinence, stromal adipocytic metaplasia, mucin deposit, prominent stromal fibrosis and vascularization, and perineural arrangement of cells (Table 2).

Immunohistochemical features

All 50 lesions manifested nuclear loss of BAP1 staining in at least a subset of melanocytic population. Conventional melanocytes with retained BAP1 nuclear expression were observed in 45 cases (90%). In many combined type BIMTs, mixed nests composed of both BAP1-negative and BAP1-positive melanocytes were seen at the dermoepidermal junction (36%) or within the dermis (54%) (Fig. 1B). Nests composed exclusively of BAP1-inactivated melanocytes were seen in half the cases. Micronuclei were always negative for BAP1 to distinguish them from lymphocytes.

Molecular results (Table 3)

BAP1 *mutation analysis and* BAP1 *(3p21.1) copy number changes.* Of the 26 lesions analyzed for *BAP1* mutations, 16 harbored a single *BAP1* mutation, 4 neoplasms yielded 2 different mutations (biallelic mutation), 4 were negative and the remaining 2 lesions were not analyzable. Two cases initially tested negative by Sanger sequencing proved subsequently positive with NGS. Novel *BAP1* mutations included NM_004656.3: c.14 G > A p.(Trp5Ter), c.25 G > T p.(Glu9Ter), c.249_250delinsT p.(His84ThrfsTer3), c.390_412del p.(Ile131GlnfsTer4), c.700 G > C p.(Val234Leu), and c.856 A > T p.(Lys286Ter) (Fig. 6).

Eight patients were tested for *BAP1* germline mutations (saliva & peripheral blood) and four proved positive. An additional patient with multiple neoplasms, in whom two tumors were tested with the MelArray, revealed an identical *BAP1* mutation (c.1717delG).

Of the 27 cases tested for *BAP1* CNVs by FISH, ten proved positive (heterozygous loss of *BAP1*), nine negative, whereas the remaining eight cases were not analyzable. Of the ten positive cases with *BAP1* loss identified by FISH, seven also harbored a *BAP1* mutation, whilst the remaining three lesions were not studied. Additionally, one of the two lesions tested for *BAP1* copy number changes by the MelArray, revealed heterozygotous loss of *BAP1*, while another did not (identical *BAP1* mutation were found in both lesions).

In combined results for *BAP1* mutations and *BAP1* CNVs, there were five lesions negative for both *BAP1* mutation and *BAP1* CNVs. Another case negative for a *BAP1* mutation was not analyzable for CNVs by FISH.

BRAF *mutation*. Among the 26 neoplasms tested for *BRAF* mutation, 24 lesions harbored $BRAF^{V600E}$ mutation.

Fusions detection. Two cases with *RAF1* fusion, namely *TRAK1-RAF1* and *IGIT2-RAF1* have been previously published[4].

Mutation analysis and studies of CNVs using NGS. In nine BIMTs, additional mutations were detected. The resulting mutational landscape is shown in (Supplementary Figure 1).

In one case (Case 7 A, 15-year-old girl), CNVs by NGS showed an isolated gain of *MYC* and in another lesion (Case 16), *FGFR1* and *ERCC2* gain were detected.

FISH for copy number changes of RRB1, CCND1, MYB, MYC*, and* CDKN2A. Of the 27 cutaneous lesions analyzed using the melanoma-specific probes, 20 were negative, 6 non-analyzable, whereas one neoplasm (Case 8) showed a gain of *MYC* and *RREB1*.

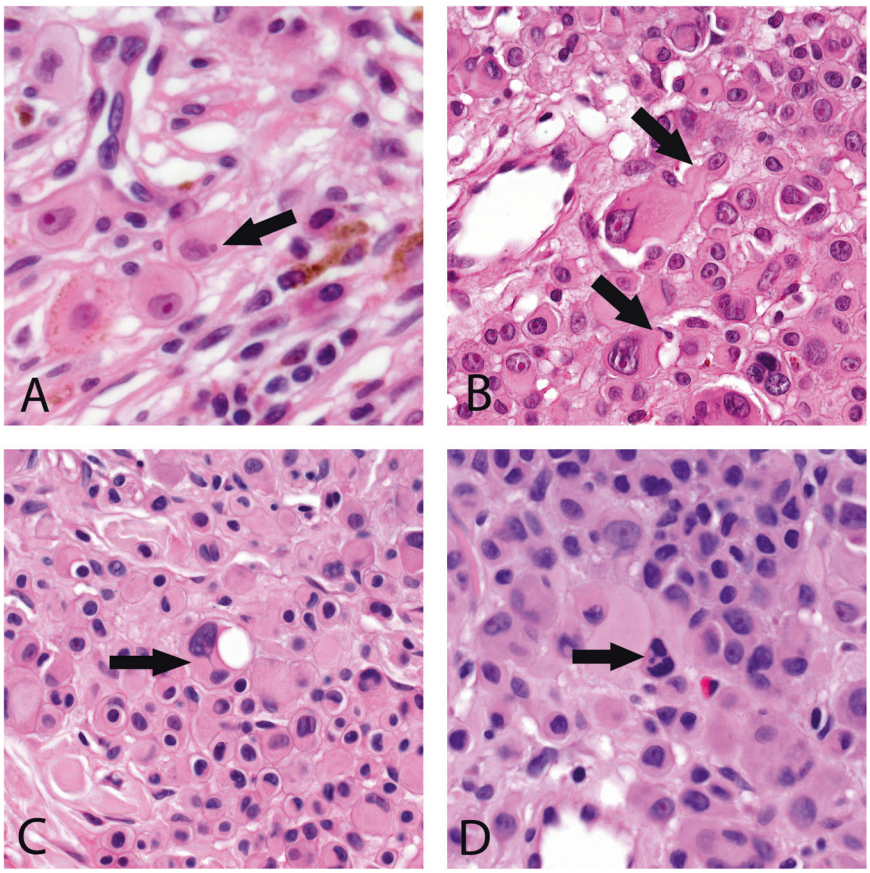

Fig. 3 Micronuclei, ant-bear cells and nuclear budding in BIMT. Micronucleus in a BAP1-inactivated melanocyte. Micronuclei are defined as a small nucleus or nuclear buds being 1/3 or smaller compared to the main nucleus presented with a similar or slightly lighter non-refractile staining intensity (arrows). They are observed in the cytoplasm of epithelioid melanocytes, as well as lying in contact with their membrane. Compare their dimension with the nucleus of a lymphocyte or plasma cell (arrowheads) (**A**). Large epithelioid melanocytes with cytoplasmic protrusions resembling proboscis (ant-bear cells). Note the micronucleus and small nucleus at the end of the protrusions (arrows) (**B**). Nuclear budding in BAP1-inactivated melanocytes. The nuclei of the epithelioid cells display extreme variability in size, shape, and stain intensity. Note nuclear buds of variable dimension detaching from the main nucleus (**C**, **D**).

Tetraploid mononuclear cells were observed in five cases, while occasional multinucleated cells resulting in overlapping nuclei were always present and showed multiple signals but were not assessed and therefore were not considered tetraploid in our series.

The lymph node lesion (Case 31C) was tested negatively.

DISCUSSION

Consistent with the prior studies, BIMTs in our series were predominately small (0.2–1.2 cm), dome-shaped or polypoid lesions occurring mainly in young patients (median age 30.4 years, for germline mutated cases 24 years) sparing the lower extremities[7,8,10,18,31,32]. In contrast to the previous studies, we found a female predominance (female to male ratio is 2.3:1).

Microscopically, a vast majority of the lesions were of combined type and were associated with a conventional melanocytic nevus frequently showing congenital-like features. In several cases, only careful evaluation of BAP1 staining and mapping with HE-stained slides allowed detection of small, scattered nests of residual conventional melanocytes retaining BAP1 nuclear expression at the periphery of the lesions. The BAP1-inactivated population was mainly located in the dermis and presented an expansile nodular pattern of growth displacing conventional melanocytes toward periphery and squeezing them beneath the overlying epidermis. At the transitional zone between the residua of the conventional nevus and epithelioid cells, the latter often focally retained the architecture of the nevus, that is a nested pattern (nests exclusively composed of BAP1-inactivated melanocytes) or single-cell files splaying between collagen bundles corresponding to a congenital pattern. Mixed nests composed of both BAP1-negative and BAP1-positive melanocytes were observed in the dermis and/or at the dermoepidermal junction in many lesions. In a few cases, BAP1-inactivated epithelioid melanocytes showed a perineural, perivascular, or periadnexal distribution. Toward the base of the lesion, BAP1-inactivated epithelioid melanocytes featured an infiltrative pattern with more dyscohesive areas, especially when accompanied by lymphocytes, and showed in some cases a deep bulb-like extension.

Taken together, all these morphological findings suggest an advantage of the growth of the BAP1-inactivated population that replaces the original conventional melanocytic one. In this view, pure type BIMTs that we encountered only in five cases (10%) may represent the end stage of the process of a clonal substitution of the original nevus cells by BAP1-inactivated melanocytes. This model of progression of BIMT from a benign nevus was proposed in the original description[8] and is also supported from a molecular viewpoint, inasmuch as both combined and pure cases in our series and in the previously reported ones[2,5,33] harbored a $BRAF^{V600E}$ mutation in the presence of *BAP1* inactivation. Moreover, combined type BIMTs have also been reported in association with an *NRAS* mutation and *RAF1* fusions[3,4,33], both known to act as a mitogenic driver in melanocytic neoplasms[34]. Fusions involving receptor tyrosine kinases and serine/threonine kinases

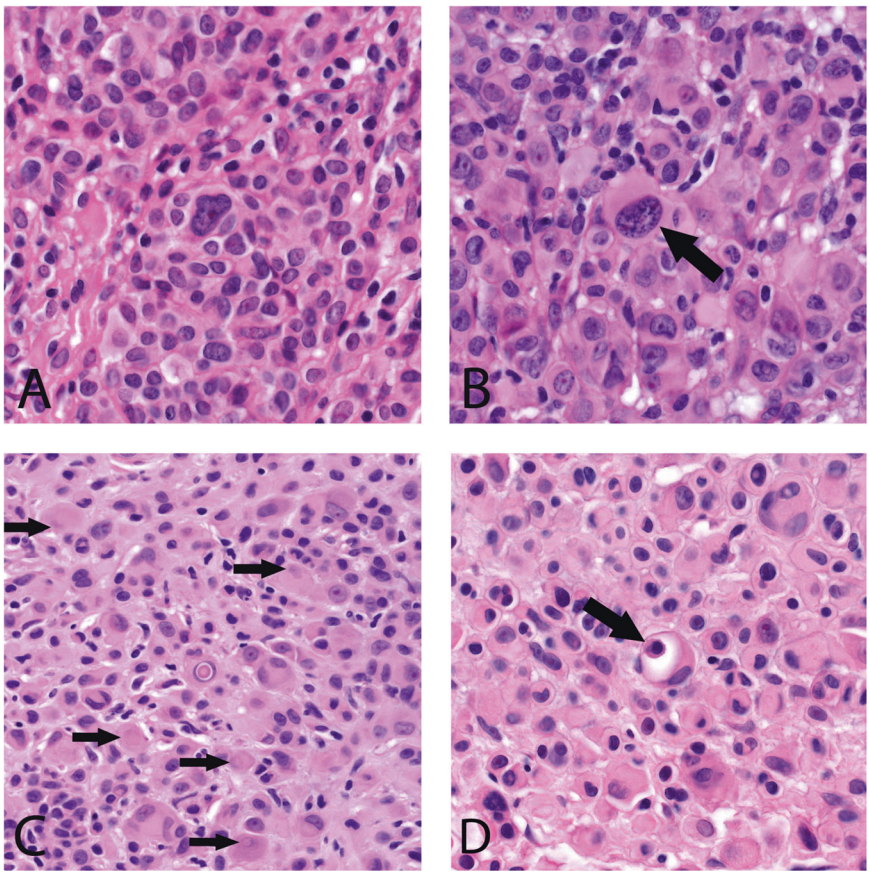

Fig. 4 Other cytological features in BIMT. Cells with large irregular nuclei resembling blebbing. Note the mosaic-like disposition of the surrounding cells (**A**). Large epithelioid melanocytes with enlarged nuclei showing clumped chromatin (arrow) (**B**). Cells are exclusively composed of large eosinophilic cytoplasm with only a shadow/vestige of a nucleus (arrows). Epithelioid melanocyte with an eosinophilic nuclear pseudoinclusion can be seen in the center (**C**). Cells with a lumina-like empty intracytoplasmic inclusion encasing small to medium-sized melanocytes occasioning a resemblance to the so-called ball-in-mitt structures. This kind of cell-in-cell structure likely represents entosis in which a tumor cell (host) contains another cell (internalized cell) that displaces the nucleus of the host cells towards the cell periphery resulting in so-called "bird"s- eye cells' morphology (arrow) (**D**).

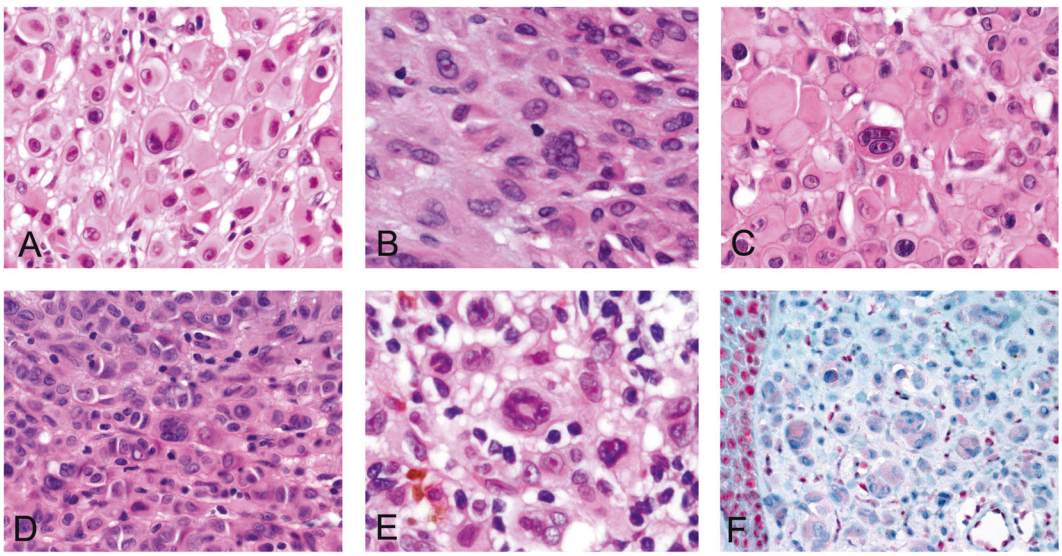

Fig. 5 Multinucleated/giant epithelioid melanocytes in BIMT. Binucleated cells resembling Reed-Sternberg cells (**A**) and multinucleated/giant cells with overlapping nuclei result in a popcorn, coin-on-a-plate, or wreath-like morphology (**B**–**E**). Note prominent eosinophilic nucleoli in the nuclei of some cells (**A**–**D**). Multinucleated/giant cell showing BAP1 nuclear loss (**F**).

are mostly associated with Spitz lesions, whereas mutations are typical for conventional melanocytic lesions. However, there are well-known exceptions such as *HRAS* mutation in desmoplastic Spitz nevus and *MAP2K1* mutations in Spitz lesions[35–37]. RAF proto-oncogene serine/threonineprotein kinase encoded by *RAF1* functions as an alternative MAPK signaling mechanism as it forms dimers with wild-type BRAF[38].

Although large epithelioid melanocytes with ample eosinophilic cytoplasm, well-demarcated cytoplasmic border represent the histological hallmark of BIMTs, extreme variability in cellular size, shapes, and degree of nuclear pleomorphism results in a remarkable intratumoral heterogeneity, which has been previously noted[33,39]. Apart from binucleated cells mentioned in the previously published material, we identified several types of multinucleated cells, resembling those seen in Hodgkin lymphoma, including Reed-Sternberg cells, popcorn cells, coin-on-a-plate cells, and mummified cells. Additionally, multinucleated cells with other appearances (floret cells, wreath-like cells) were noted. The question arises as to how one can explain this remarkable cellular heterogeneity and pleomorphism. Taking into account the clonal expansion of epithelioid melanocytes characterized by the loss of a tumor suppressor gene *BAP1* (the second genetic event) in a pre-existing conventional melanocytic nevus driven by a constitutively active mitogenic mutation (i.e. *BRAF*, primary genetic event), it seems reasonable to consider BIMTs a clonal model of tumor progression of melanoma from a pre-existing nevus. However, the indolent clinical behavior in most cases argues against this interpretation. In addition, lesions with loss of BAP1 nuclear expression and no biallelic inactivation of *BAP1* on molecular analysis identified by others and us suggest, among others, epigenetic changes that may account for the inactivation of the *BAP1* gene[5]. A recent study demonstrated global transcriptional reprogramming during the progression of BIMTs comparing the gene expression profiles of *BRAF*-driven/*BAP1*-inactivated epithelioid melanocytes with the adjacent conventional melanocytic population[40].

Part of the cellular features in BIMTs can be related to cellular senescence that supposedly occurs early in this progression. Among them is multinucleation that is commonly encountered in conventional melanocytic nevi and less frequently in borderline lesions and overt melanomas[41–44].

Despite high cellularity and expansile growth, others and we noted a relatively low mitotic activity. Peculiar chromatin patterns ranged from open (shadow nuclei) to clumped. Multinucleated wreath-like/floret-like/coin-on-a-plate cells and micronuclei may result from nuclear budding (Fig. 3C, D). In addition, nuclear budding with the internal perinuclear membrane wrapping around singular nuclei facilitating peculiar nuclear pseudoinclusions observed by others and us[15,45]. On the whole, the extreme variability in cellular size and morphology may represent the expression of maturation and differentiation of small epithelioid cells (Fig. 7).

Our FISH analysis revealed tetraploidy in 5 of the 21 cases studied. Generally, FISH analysis is based on a threshold of positive cells and usually tends to scotomize scattered polyploid nuclei. In 2011, before the recognition of BIMT as a distinct lesion, Pouryazdanparast et al. reported tetraploid cells as a common feature in a proportion of nevi with an "atypical spitzoid epithelioid component"[46]. The authors postulated that as a result of senescent mechanisms that are activated, these cells become trapped in the tetraploid cell and do not undergo further division, thus linking senescent or ancient features with tetraploidy. Of further note, they reported that polyploidy changes were noticed only in cases with a low mitotic count. The pictures shown by the authors present the typical morphological features of BIMTs (Fig. 1B, D in ref. [46]). It has been recently observed that compared to conventional melanocytic nevi, BIMTs have decreased ciliation and increased centrosome amplification, further linking BAP1 dysfunction to mitotic abnormalities and chromosomal instability[47]. Amplification of centrosome number has been shown to occur through failure to arrest at a G_1 tetraploidy checkpoint after failure to segregate the genome in mitosis[48].

To the best of our knowledge, the only documented case of BIMT with an aggressive clinical course was reported by Aung et al.[17] and the neoplasm was composed of atypical but rather nevoid melanocytes with BAP1 loss.

Prior case series of BIMTs had a relatively short mean follow-up (17 months)[49,50]. Of the 21 patients with available follow-up in our

Table 3. Summary of the genetic data on BIMTs.

Gene	Frequency
BRAF V600E	24/26
RAF1 fusion	2/14
BAP1 biallelic mutation	4/22
BAP1 single allele mutation	16/24
BAP1 germline mutation	5/9[a]
BAP1 heterozygous loss	11/22
FISH for RRB1, CCND1, MYB, MYC, CDKN2A	1/21[b]
TERT-p mutation	0/14
Copy number variations (NGS)	2/8[c]
Tetraploid mononuclear cells	5/21

[a]In four patients, a germline *BAP1* mutation was detected using blood or saliva, while in the remaining one patient identical *BAP1* mutations were seen in different lesions, strongly suggesting a germline mutation.
[b]One tumor showed *RREB1* and *MYC* gain.
[C]One tumor revealed *MYC* gain, another *FGFR1* and *ERCC2* gains.

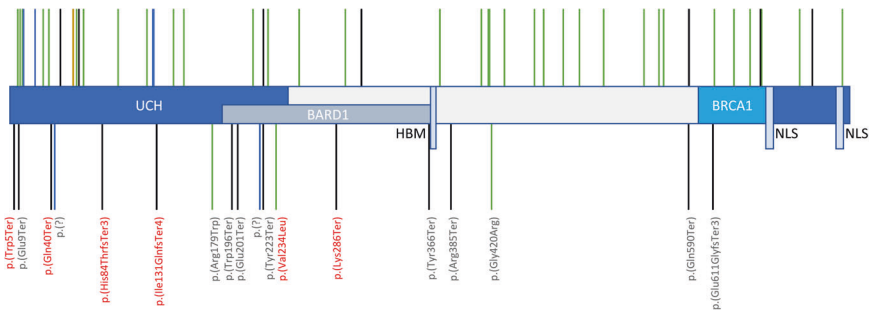

Fig. 6 *BAP1* mutations identified in our study. BAP1 diagram with protein domains. *UCH* Ubiquitin C-terminal hydrolase, *HBM* Host cell factor C1 binding motif, *NLS* Nuclear localization signal, *BARD1* BRCA1-associated RING domain protein 1 gene binding domain, *BRCA1* BR CA1 gene binding domain. **A** Published mutation in skin neoplasms in TCGA database–green lines = missense mutations, black lines = truncating mutations, brown line = small deletion. **B** Mutations found in this study–red text of mutation name = novel mutation, blue line = splicing mutation, black line = truncating mutation, green line = missense mutation.

series, only one patient did develop a locoregional lymph node metastasis 6 years after the removal of the primary tumor. The patient was a 7-year-old girl with a lesion located on the neck, had a considerable lymphocytic infiltrate, and showed relatively bland cytological features; binucleated and multinucleated cells were absent. The neoplasm was diagnosed as a nevus. Six years later (at the age of 13), she developed an enlarged lymph node under her scapula 5 cm from the previously removed skin lesion, and its biopsy demonstrated a dense infiltrate of small to large epithelioid melanocytic cells substituting the original lymphoid tissue. No other melanocytic lesion was known to be excised in between. After having received a second skin biopsy 2 years later in which a classical combined BIMT with remnants of a nevus and epithelioid melanocytes were seen, the original skin lesion and the lymph node specimen were retrospectively stained for BAP1. Loss of BAP1 nuclear expression was found in both specimens, with diffuse nuclear negativity in the skin lesion (Fig. 8). Of note, in the tumor reported by Wiesner et al.[13], melanoma arising in BIMT manifested larger nuclei compared with the rest of the neoplasm but featured no striking pleomorphism to our eye and both melanoma and nevus showed loss of BAP1 nuclear expression by immunohistochemistry. Recently, cases of *BAP1*-inactivated melanocytic tumors showing a conventional morphology in the absence of the classical epithelioid component have been reported[19,20]. To explain this phenomenon the authors postulated a time gap between genotype alterations and phenotype manifestations related to progressive intracellular accumulation of the BAP1-altered protein in the affected melanocytes. Moreover, *BAP1*-inactivated tumors with a conventional morphology were frequently observed in younger patients harboring *BAP1* germline mutation[20]. Apart from the above-mentioned patient with a lymph node metastasis, we observed this histological presentation in other two lesions, each from a different patient. Both had multiple lesions and either family or personal history of cutaneous melanoma. In one of these two patients, germline mutation could not be studied, whereas in the other patient an identical *BAP1* mutation was found in two different neoplasms, strongly suggesting a germline mutation. Of note, one lesion from this patient manifested features of a conventional nevus with conspicuous dysplastic-like changes.

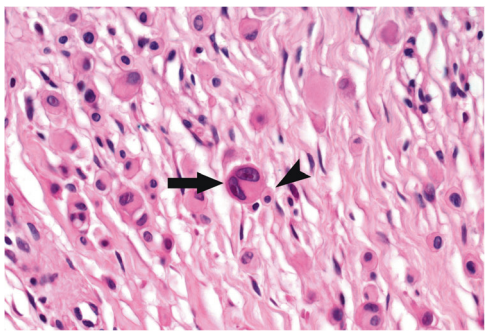

Fig. 7 Extreme variability in cellular size and morphology in BIMT. Note a small epithelioid melanocyte (arrowhead), lying in contact with the cell membrane of binucleated cells with prominent nucleoli resembling Read-Sternberg cell (arrow). The neoplasm showed a pure morphology and inverse maturation with predominant small epithelioid cells growing in an infiltrative fashion at the periphery of the lesion. Amplification of both *RREB1* and *MYC* was detected by FISH in this case.

Our genetic study revealed several findings that merit comment. We identified six novel, previously unreported *BAP1* mutations. All of these represent frame-shift mutations located in, or shortly after, the ubiquitin C-terminal hydrolase domain, causing truncation of parts of the domain and the rest of the protein, resulting in the loss of the protein's function. There were 5 cases in which neither *BAP1* mutation nor heterozygous loss of the *BAP1* gene was found, and there was a further case negative for *BAP1* mutation but not analyzable for CNVs. Since biallelic inactivation of *BAP1* is generally accepted to be required for BAP1 protein loss, these missing aberrations could be attributed either to a *BAP1* aberration outside the studied region, or to other unknown mechanisms of BAP1 loss. Noteworthy was an 11-year-

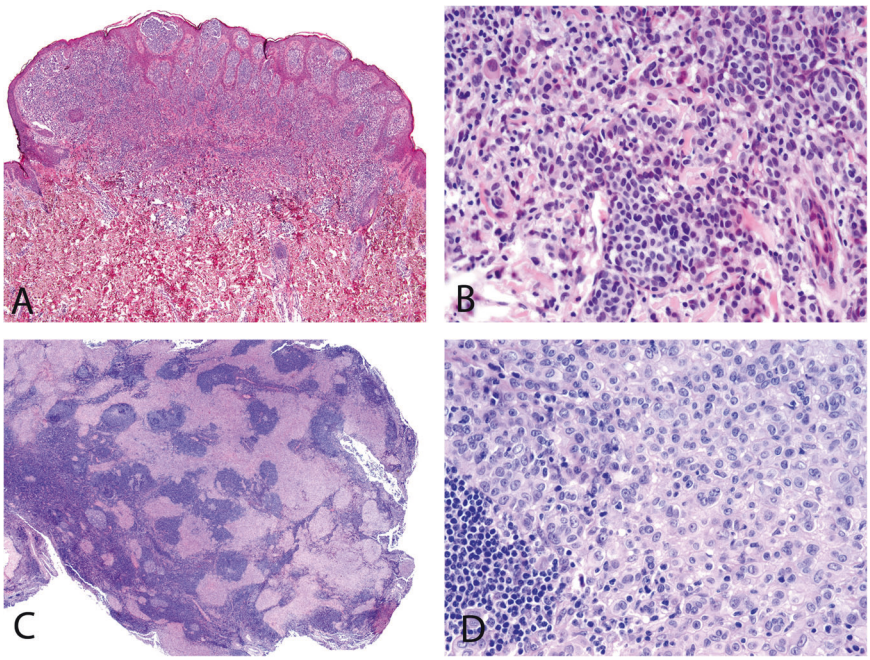

Fig. 8 Histological presentation of cutaneous BIMT of a 7-year-old girl and lymph node metastasis. Microscopically, the lesion was of the pure type and showed relatively bland cytological features without binucleated and multinucleated cells (**A**, **B**). A lymph node lesion. Note a dense infiltrate of small to large epithelioid melanocytic cells substituting the original lymph node tissue and characterized by BAP1 nuclear loss (not shown) (**C**, **D**).

old girl with multiple lesions located predominantly on the back and extremities. All five lesions manifested typical features of BIMT with nuclear loss of BAP1 expression in the epithelioid melanocytes on immunohistochemistry. Her peripheral blood tested negative for *BAP1* mutation, as did two BIMTs. In addition, neither of the studied cutaneous neoplasms showed CNVs of *BAP1*.

Apart from *BAP1*, DNA and RNA sequencing detected several mutations in other genes; the effects of these alterations in this setting are unknown. However, in one case (Case 1 A, 11-year-old girl with multiple lesions and family history of similar lesions), one of the neoplasms yielded a relatively high number of mutations, including a *POLE* mutation, compared to the rest of the analyzed cases. The detected *POLE* mutation has been linked to high TMB[51]. The panels used in our study are not large enough to be able to access TMB accurately, however, the presence of a *POLE* mutation and a high number of mutations are indicative of high TMB. Microscopically, the neoplasm displayed only minimal residual conventional melanocytes while prominent giant epithelioid melanocytes with clumped chromatin. The patient is disease-free after 51 months of follow-up.

A recent study revealed two cases of BIMTs with FISH for copy number variations in melanoma-related genes such as 6p25 (*RRB1*), 11q13 (*CCND1*), and 9p21 (*CDKN2A*)[17]. In our series, only 1 out of the 21 analyzable lesions (Case 8, a 67-year-old man) did disclose amplification of both *RREB1* and *MYC*. This neoplasm showed a pure morphology and inverse maturation with predominant small epithelioid cells growing in an infiltrative fashion at the periphery of the lesion. The patient died of an unrelated cause after an otherwise unremarkable follow-up of 72 months. In another case (Case 7 A, 15-year-old girl), copy number variation by NGS showed an isolated gain of *MYC* gene. Also, in this case, we observed only a minimal residuum of conventional melanocytes. Unfortunately, the follow-up of the patient is not available.

This is the first study that has investigated mutations in the promoter region of the *TERT* gene (*TERT-p*), using an NGS panel. *TERT-p* hot-spot mutations have been associated with an aggressive clinical course in melanocytic neoplasms, especially in cases with ambiguous morphological features/borderline or low-grade tumors[52,53]. None of the 14 neoplasms successfully sequenced harbored an alteration in the *TERT-p* region.

In conclusion, our study of a large series of BIMTs extends their morphological spectrum and report novel *BAP1* mutations. BIMTs appear to represent a progression from a conventional senescent melanocytic nevus but certain microscopic features, together with cases without detectable molecular alteration in *BAP1* gene and frequent tetraploidy, suggest more complex underlying pathological events, which needs to be studied. Albeit BIMTs may present with several alarming cytological and architectural features, we confirm an indolent clinical course in most cases; however, follow-up was relatively short. The only metastatic case in our series was a child with a nevoid-like lesion with a pure morphology showing relatively bland cytological features. This relatively bland morphology was similar to that seen in a few previously reported cases as melanoma with *BAP1* inactivation[13,17]. The working group of the WHO classification suggests the term melanocytoma for "atypical combined tumors (that) may be potential precursor lesions of melanoma" but some atypia is seen in almost all cases of BIMTs that rarely, if ever progress to melanoma. From a genetic viewpoint, according to the WHO classification, the term melanocytoma appears to be restricted for atypical combined melanocytic lesions with two distinctive genetic alterations. Yet, Yeh applied the designation melanocytoma for atypical Spitz tumor which does not have two critical genetic events[54]. Further studies are needed to define and characterize melanocytoma and study BIMTs with relatively bland (nevoid-like) cytology and adverse clinical events.

DATA AVAILABILITY

All original data are available per request.

REFERENCES

1. Elder, D. E., Massi, D., Scolyer, R. A., Willemze, R. & eds. WHO Classification of Skin Tumours. 4th edn. *Lyon, France: International Ag*ency for Research on Cancer (IARC) (2018).
2. Busam, K. J., Sung, J., Wiesner, T., von Deimling, A. & Jungbluth, A. Combined BRAF(V600E)-positive melanocytic lesions with large epithelioid cells lacking BAP1 expression and conventional nevomelanocytes. *Am. J. Surg. Pathol.* **37**, 193–199 (2013).
3. Blokx, W. A. et al. NRAS-mutated melanocytic BAP1-associated intradermal tumor (MBAIT): a case report. *Virchows Arch.* **466**, 117–121 (2015).
4. Donati, M. et al. RAF1 gene fusions as a possible driver mechanism in rare BAP1-inactivated melanocytic tumors: a report of 2 cases. *Am. J. Dermatopathol.* **42**, 961–966 (2020).
5. Wiesner, T. et al. A distinct subset of atypical Spitz tumors is characterized by BRAF mutation and loss of BAP1 expression. *Am. J. Surg. Pathol.* **36**, 818–830 (2012).
6. Shain, A. H. et al. The genetic evolution of melanoma from precursor lesions. *N. Engl. J. Med.* **373**, 1926–1936 (2015).
7. Garfield, E. M. et al. Histomorphologic spectrum of germline-related and sporadic BAP1-inactivated melanocytic tumors. *J. Am. Acad. Dermatol.* **79**, 525–534 (2018).
8. Wiesner, T. et al. Germline mutations in BAP1 predispose to melanocytic tumors. *Nat. Genet.* **43**, 1018–1021 (2011).
9. Abdel-Rahman, M. H. et al. Germline BAP1 mutation predisposes to uveal melanoma, lung adenocarcinoma, meningioma, and other cancers. *J. Med. Genet.* **48**, 856–859 (2011).
10. Njauw, C. N. et al. Germline BAP1 inactivation is preferentially associated with metastatic ocular melanoma and cutaneous-ocular melanoma families. *PLoS One* **7**, e35295 (2012).
11. Popova, T. et al. Germline BAP1 mutations predispose to renal cell carcinomas. *Am. J. Hum. Genet.* **92**, 974–980 (2013).
12. Testa, J. R. et al. Germline BAP1 mutations predispose to malignant mesothelioma. *Nat. Genet.* **43**, 1022–1025 (2011).
13. Wiesner, T. et al. Toward an improved definition of the tumor spectrum associated with BAP1 germline mutations. *J. Clin. Oncol.* **30**, e337–e340 (2012).
14. Ardakani, N. M., Palmer, D. L. & Wood, B. A. BAP1 deficient malignant melanoma arising from the intradermal component of a congenital melanocytic naevus. *Pathology* **47**, 707–710 (2015).
15. Marušić, Z., Buljan, M. & Busam, K. J. Histomorphologic spectrum of BAP1 negative melanocytic neoplasms in a family with BAP1-associated cancer susceptibility syndrome. *J. Cutan. Pathol.* **42**, 406–412 (2015).
16. Gerami, P. et al. Multiple cutaneous melanomas and clinically atypical moles in a patient with a novel germline BAP1 mutation. *JAMA Dermatol.* **151**, 1235–1239 (2015).
17. Aung, P. P. et al. Melanoma with loss of BAP1 expression in patients with no family history of bap1-associated cancer susceptibility syndrome: a case series. *Am. J. Dermatopathol.* **41**, 167–179 (2019).
18. Carbone, M. et al. BAP1 cancer syndrome: malignant mesothelioma, uveal and cutaneous melanoma, and MBAITs. *J. Transl. Med.* **10**, 179 (2012).
19. Wysozan, T. R., Khelifa, S., Turchan, K. & Alomari, A. K. The morphologic spectrum of germline-mutated BAP1-inactivated melanocytic tumors includes lesions with conventional nevic melanocytes: a case report and review of literature. *J. Cutan. Pathol.* **46**, 852–857 (2019).
20. Louw, A. et al. Histologically diverse BAP1-deficient melanocytic tumors in a patient with BAP1 tumor predisposition syndrome. *Am. J. Dermatopathol.* **42**, 872–875 (2020).
21. Foretová, L. et al. BAP1 syndrome - predisposition to malignant mesothelioma, skin and uveal melanoma, renal and other cancers. *Klin. Onkol.* **32**, 118–122 (2019).
22. Donati, M. et al. Spitz tumors with ROS1 fusions: a clinicopathological study of 6 cases, including FISH for chromosomal copy number alterations and mutation analysis using next-generation sequencing. *Am. J. Dermatopathol.* **42**, 92–102 (2020).
23. Šteiner, P., Pavelka, J., Vaneček, T., Miesbauerová, M. & Skálová, A. Molecular methods for detection of prognostic and predictive markers in diagnosis of adenoid cystic carcinoma of the salivary gland origin. *Cesk. Patol.* **54**, 132–136 (2018).
24. Švajdler, M. et al. Fibro-osseous pseudotumor of digits and myositis ossificans show consistent COL1A1-USP6 rearrangement: a clinicopathological and genetic study of 27 cases. *Hum. Pathol.* **88**, 39–47 (2019).
25. Lek, M. et al. Analysis of protein-coding genetic variation in 60,706 humans. *Nature* **536**, 285–291 (2016).
26. Landrum, M. J. et al. ClinVar: improving access to variant interpretations and supporting evidence. *Nucleic Acids Res.* **46**, D1062–D1067 (2018).

27. Hilbers, M. L. et al. Standardized diagnostic algorithm for spitzoid lesions aids clinical decision-making and management: a case series from a Swiss reference center. *Oncotarget* **12**, 125–130 (2021).
28. Gerami, P. et al. A highly specific and discriminatory FISH assay for distinguishing between benign and malignant melanocytic neoplasms. *Am. J. Surg. Pathol.* **36**, 808–817 (2012).
29. Michal, M. Cellular blue naevi with microalveolar pattern-a type of naevus frequently confused with melanoma. *Pathol. Res. Pract.* **194**, 83–86 (1998).
30. Kazakov, D. V. & Michal, M. Melanocytic "ball-in-mitts" and "microalveolar structures" and their role in the development of cellular blue nevi. *Ann. Diagn. Pathol.* **11**, 160–175 (2007).
31. Piris, A., Mihm, M. C. Jr. & Hoang, M. P. BAP1 and BRAFV600E expression in benign and malignant melanocytic proliferations. *Hum. Pathol.* **46**, 239–245 (2015).
32. Haugh, A. M. et al. Genotypic and phenotypic features of BAP1 cancer syndrome: a report of 8 new families and review of cases in the literature. *JAMA Dermatol.* **153**, 999–1006 (2017).
33. Yeh, I. et al. Ambiguous melanocytic tumors with loss of 3p21. *Am. J. Surg. Pathol.* **38**, 1088–1095 (2014).
34. Hayward, N. K. et al. Whole-genome landscapes of major melanoma subtypes. *Nature* **545**, 175–180 (2017).
35. Bastian, B. C., LeBoit, P. E. & Pinkel, D. Mutations and copy number increase of HRAS in Spitz nevi with distinctive histopathological features. *Am. J. Pathol.* **157**, 967–972 (2000).
36. Sunshine, J. C. et al. Melanocytic neoplasms with MAP2K1 in frame deletions and spitz morphology. *Am. J. Dermatopathol.* **42**, 923–931 (2020).
37. Donati, M. et al. MAP2K1-mutated melanocytic neoplasms with a SPARK-like morphology. *Am. J. Dermatopathol.* **43**, 412–417 (2021).
38. Lavoie, H. & Therrien, M. Regulation of RAF protein kinases in ERK signalling. *Nat. Rev. Mol. Cell Biol.* **16**, 281–298 (2015).
39. Llamas-Velasco, M., Pérez-Gónzalez, Y. C., Requena, L. & Kutzner, H. Histopathologic clues for the diagnosis of Wiesner nevus. *J. Am. Acad. Dermatol.* **70**, 549–554 (2014).
40. Webster, J. D. et al. The tumor suppressor BAP1 cooperates with BRAFV600E to promote tumor formation in cutaneous melanoma. *Pigment Cell Melanoma Res.* **32**, 269–279 (2019).
41. Gray-Schopfer, V. C. et al. Cellular senescence in naevi and immortalisation in melanoma: a role for p16? *Br. J. Cancer.* **95**, 496–505 (2006).
42. Michaloglou, C. et al. BRAFE600-associated senescence-like cell cycle arrest of human naevi. *Nature* **436**, 720–724 (2005).
43. Saggini, A. et al. Uncommon histopathological variants of malignant melanoma. Part 2. *Am. J. Dermatopathol.* **41**, 321–342 (2019).
44. Houlier, A. et al. Melanocytic tumors with MAP3K8 fusions: report of 33 cases with morphological-genetic correlations. *Mod. Pathol.* **33**, 846–857 (2020).
45. O'Shea, S. J. et al. Histopathology of melanocytic lesions in a family with an inherited BAP1 mutation. *J. Cutan. Pathol.* **43**, 287–289 (2016).
46. Pouryazdanparast, P., Haghighat, Z., Beilfuss, B. A., Guitart, J. & Gerami, P. Melanocytic nevi with an atypical epithelioid cell component: clinical, histopathologic, and fluorescence in situ hybridization findings. *Am. J. Surg. Pathol.* **35**, 1405–1412 (2011).
47. Ye, J., Sheahon, K. M., LeBoit, P. E., McCalmont, T. H. & Lang, U. E. BAP1-inactivated melanocytic tumors demonstrate prominent centrosome amplification and associated loss of primary cilia. *J. Cutan. Pathol.* **8**, 1353–1360 (2021).
48. Borel, F., Lohez, O. D., Lacroix, F. B. & Margolis, R. L. Multiple centrosomes arise from tetraploidy checkpoint failure and mitotic centrosome clusters in p53 and RB pocket protein-compromised cells. *Proc. Natl. Acad. Sci. USA* **99**, 9819–9824 (2002).
49. Fischer, A. S. & High, W. A. The difficulty in interpreting gene expression profiling in BAP-negative melanocytic tumors. *J. Cutan. Pathol.* **45**, 659–666 (2018).
50. Gammon, B., Traczyk, T. N. & Gerami, P. Clumped perinuclear BAP1 expression is a frequent finding in sporadic epithelioid Spitz tumors. *J. Cutan. Pathol.* **40**, 538–542 (2013).
51. Hühns, M. et al. High mutational burden in colorectal carcinomas with monoallelic POLE mutations: absence of allelic loss and gene promoter methylation. *Mod. Pathol.* **33**, 1220–1231 (2019).
52. Lee, S. et al. TERT promoter mutations are predictive of aggressive clinical behavior in patients with spitzoid melanocytic neoplasms. *Sci. Rep.* **5**, 11200 (2015).
53. Cohen, J. N., Yeh, I., Mully, T. W., LeBoit, P. E. & McCalmont, T. H. Genomic and clinicopathologic characteristics of PRKAR1A-inactivated melanomas: toward genetic distinctions of animal-type melanoma/pigment synthesizing melanoma. *Am. J. Surg. Pathol.* **44**, 805–816 (2020).
54. Yeh, I. New and evolving concepts of melanocytic nevi and melanocytomas. *Mod. Pathol.* **33**, 1–14 (2020).

AUTHOR CONTRIBUTIONS

All authors contributed to the study and manuscript preparation to justify coauthorship.

FUNDING

No funding is involved in financing the study.

COMPETING INTERESTS

The authors declare no competing interests.

ADDITIONAL INFORMATION

Supplementary information The online version contains supplementary material available at https://doi.org/10.1038/s41379-021-00976-7.

Correspondence and requests for materials should be addressed to Dmitry V. Kazakov.

Reprints and permission information is available at http://www.nature.com/reprints

Publisher's note Springer Nature remains neutral with regard to jurisdictional claims in published maps and institutional affiliations.